

# **DeepCatch-Derived Body Composition Metrics for Noninvasive Prediction of MASLD Subtypes, Fibrosis, and Liver-Related Outcomes**

Dong Hyun Kim<sup>1\*</sup>, Na Hyun Cho<sup>1\*</sup>, Hye Won Lee<sup>2-4</sup>

<sup>1</sup> Yonsei University College of Medicine, Seoul, Korea

<sup>2</sup> Department of Internal Medicine, Yonsei University College of Medicine, Seoul, Korea

<sup>3</sup> Institute of Gastroenterology, Yonsei University College of Medicine, Seoul, Korea

<sup>4</sup> Yonsei Liver Center, Severance Hospital, Seoul, Korea

\*These authors contributed equally to this work.

## **Corresponding authors**

Hye Won Lee, M.D., Ph.D.

Department of Internal Medicine, Yonsei University College of Medicine

50-1 Yonsei-ro, Seodaemun-gu, Seoul, 03722, South Korea

Tel: +82-2-2228-2288, E-mail: [lorry-lee@yuhs.ac](mailto:lorry-lee@yuhs.ac)

**Manuscript word count:** 2,132

**Total number of figures and tables:** 4 figures, 1 table (Supplementary: 2 figures, 1 table)

**Abbreviations:**

## **Abstract**

**Background/Objectives:**

**Methods:**

**Results:**

**Conclusion:**

**Abstract word count:**

**Keywords:**

## Introduction

The global burden of metabolic dysfunction-associated steatotic liver disease (MASLD), formerly known as non-alcoholic fatty liver disease (NAFLD), is rapidly rising in parallel with increasing rates of obesity and type 2 diabetes, with adult prevalence projected to exceed 55% by 2040 [1]. MASLD presents significant diagnostic challenges, particularly in identifying patients with metabolic dysfunction-associated steatohepatitis (MASH), the progressive and clinically significant form of the disease. While liver biopsy remains the gold-standard for diagnosing MASH and staging liver fibrosis, its invasiveness, cost, risk of complications, and sampling variability limit its utility in widespread clinical practice [2, 3].

Among non-invasive approaches, ultrasound-based imaging is commonly regarded as the clinical standard for initial evaluation of hepatic steatosis [4]. However, its diagnostic performance may be limited in individuals with high visceral adiposity, as ultrasound may not adequately capture the full spectrum of disease severity in these patients [5]. In contrast, cross-sectional imaging modalities such as computed tomography (CT) and magnetic resonance imaging (MRI) offer higher sensitivity and reproducibility in quantifying liver fat and evaluating abdominal body composition.

Recently, Deep Learning based software such as DeepCatch have emerged, enabling automated extraction and analysis of CT-derived body composition metrics—including visceral fat area (VFA), skeletal muscle area (SMA), and liver–spleen attenuation and volume—within seconds. In this study, we aim to evaluate whether DeepCatch-generated CT biomarkers can serve as reliable surrogates for non-invasive diagnosis of MASLD phenotypes, including steatosis severity and fibrosis staging, offering a potential alternative to invasive liver biopsy.

This study aims not only to validate DeepCatch-derived metrics against established clinical benchmarks but also to assess their clinical utility in redefining non-invasive standards for MASLD diagnosis and monitoring in the era of precision medicine.

## Methods

### Patient Selection

This retrospective study included patients who underwent abdominal computed tomography (CT) imaging between March 2006 and July 2023. The date of the CT scan was used as the reference point for deriving body composition metrics using DeepCatch, an automated image-processing software.

Patients were eligible for inclusion if they had available CT imaging along with corresponding laboratory or FibroScan data obtained within 1 year and 3 months of the CT date. Liver biopsy results and clinical information were reviewed to determine eligibility. Patients were excluded if they lacked definitive liver pathology or had liver disease attributed to non-metabolic etiologies such as viral hepatitis, cholestatic liver disease, or hepatic injury unrelated to metabolic dysfunction.

For liver-related event (LRE) analysis, the LRE date was defined as the time difference between the CT scan and the earliest documented event (ascites, variceal bleeding, hepatic encephalopathy, hepatorenal syndrome, or liver transplantation). For patients without an event, the duration from CT to the last follow-up was used.

### Study Design

CT images were analyzed using DeepCatch, which automatically identifies the third lumbar vertebral (L3) level and sets the region of interest from the lower ribs to the iliac crest.

The software quantifies adipose tissue, skeletal muscle, and organ characteristics using both cross-sectional areas at the L3 level and volumetric data across multiple slices. Visceral and subcutaneous adipose tissue were measured by area (cm<sup>2</sup>) and volume (cm<sup>3</sup>), and their attenuation in Hounsfield Units (HU) was used to assess fat quality. Skeletal muscle area and muscle attenuation were similarly assessed at the L3 level.

Liver and spleen attenuation values were obtained from precontrast CT scans, and the liver-to-spleen

attenuation ratio was calculated as a surrogate marker for hepatic fat accumulation. Liver and spleen volumes were measured using multi-slice segmentation.

All area-based metrics were normalized by height squared ( $\text{cm}^2/\text{m}^2$ ), generating indices such as the visceral fat index (VFI) and skeletal muscle index (SMI). While DeepCatch supports all CT phases, precontrast images were used for attenuation analyses to ensure consistency with prior literature. Area and volume measurements are considered stable across imaging phases.

A composite metric—adjusted visceral fat index ( $\text{VFI} - 0.44 \times \text{visceral fat volume}$ )—was developed to incorporate both fat quantity and distribution and improve its predictive value for fibrosis and long-term outcomes.

### **Stratification of BMI, LSM, and FIB-4**

To facilitate stratified analysis, body mass index (BMI), liver stiffness measurement (LSM), and FIB-4 were categorized into clinically relevant groups.

BMI was classified into six categories: underweight ( $<18.5 \text{ kg/m}^2$ ), normal ( $18.5\text{--}24.9 \text{ kg/m}^2$ ), overweight ( $25.0\text{--}29.9 \text{ kg/m}^2$ ), class I obesity ( $30.0\text{--}34.9 \text{ kg/m}^2$ ), class II obesity ( $35.0\text{--}39.9 \text{ kg/m}^2$ ), and class III obesity ( $\geq 40.0 \text{ kg/m}^2$ ).

LSM was categorized into fibrosis stages: F0 ( $<5.5 \text{ kPa}$ ), F1 ( $5.5\text{--}6.9 \text{ kPa}$ ), F2 ( $7.0\text{--}9.4 \text{ kPa}$ ), F3 ( $9.5\text{--}12.4 \text{ kPa}$ ), and F4 ( $\geq 12.5 \text{ kPa}$ ).

FIB-4 was grouped into low risk ( $<1.45$ ), intermediate risk ( $1.45\text{--}3.25$ ), and high risk ( $>3.25$ ).

### **Endpoints**

The study evaluated four primary outcomes:

1. Classification of MASLD vs no MASLD

2. Identification of moderate-to-severe steatosis (steatosis score  $\geq 2$ )
3. Prediction of advanced fibrosis (stage  $\geq 3$ )
4. Time to LRE, defined as the first occurrence of ascites, variceal bleeding, hepatic encephalopathy, hepatorenal syndrome, or liver transplantation.

### **Statistical Analyses**

All analyses were performed using Python. For classification outcomes (MASLD type, steatosis severity, fibrosis stage), receiver operating characteristic (ROC) curves were used to evaluate the predictive performance of DeepCatch-derived metrics. Area under the curve (AUC) values were reported, and optimal cutoffs were determined using Youden's J statistic.

For time-to-event analysis of LREs, Kaplan–Meier survival curves were generated and compared using log-rank tests. Univariable and multivariable Cox proportional hazards models were used to estimate hazard ratios (HRs). Statistical significance was defined as two-sided p-value  $< 0.05$ .

## Results

### Patients

A total of 292 patients who underwent abdominal CT imaging and evaluation using the DeepCatch program, along with available liver biopsy results, were initially screened. Seven patients were excluded due to the absence of definitive liver pathology findings. The remaining 285 patients without cancer-related biopsy results were considered eligible for analysis. Of these, 63 were excluded due to liver disease of non-metabolic etiology, including injury-related, chronic viral, or cholestatic hepatitis. Ultimately, 229 patients with complete DeepCatch-derived metrics and biopsy-confirmed histological data were included in the final analysis (**Figure 1**).

The follow-up duration, defined as the time from baseline CT or FibroScan date to the last follow-up or LRE, had a median of 65.1 months (IQR: 46.2–113.3 months). Baseline characteristics for the overall cohort and stratified comparisons between advanced and non-advanced fibrosis groups are summarized in **Table 1**.

### Distribution of Traditional and DeepCatch-Derived Metrics Across MASLD Subtypes

We compared the distribution of both traditional and DeepCatch-derived metrics across the four MASLD categories (None, MASLD, MASH, and Cirrhosis). Fibrosis-related markers such as LSM and FIB-4 demonstrated a progressively increasing trend across the disease spectrum, with values rising from None to MASLD, MASH, and peaking in Cirrhosis (**Figure 2**). This gradient reinforces their established role as indicators of fibrosis severity.

In contrast, steatosis-related metrics—including BMI, CAP, visceral fat area, and the liver-to-spleen attenuation ratio (Liver/Spleen HU)—exhibited non-linear, U-shaped or inverse U-shaped distributions. These variables increased from the None group to MASH but declined in patients with cirrhosis. Additional DeepCatch-derived metrics shown in **Supplementary Figure 1**, including liver attenuation, liver PDFF, subcutaneous fat area, and visceral fat area demonstrated similar U- or inverse U-shaped

distributions across disease stages. This pattern aligns with known histological regression of hepatic steatosis in advanced fibrosis due to hepatocyte dropout, altered lipid metabolism, and fibrotic remodeling.

### **Prediction of MASLD Type**

To evaluate the performance of DeepCatch-derived metrics in distinguishing MASLD from non-MASLD, we conducted ROC analysis using histological classification as the reference standard (**Figure 3A**). Among evaluated features, visceral fat area demonstrated the highest predictive performance with an AUC of 0.764, outperforming CAP (0.720) and BMI (0.744). For visceral fat area, the best cutoff was 108.59, yielding an accuracy of 80.3%, precision of 0.971, recall of 0.809, and an F1-score of 0.883. Other well-performing DeepCatch metrics included Liver/Spleen HU (0.739), visceral fat index (0.730), and total fat index (0.724).

### **Prediction of Steatosis Severity**

We next assessed the ability of imaging-based metrics to predict moderate-to-severe steatosis (score  $\geq 2$ ) based on histology (**Figure 3B**). Liver/Spleen HU showed the strongest performance (AUC = 0.815), exceeding liver HU (0.771), PDFF (0.769), and CAP (0.714). BMI (0.599) and categorical BMI (0.581) showed limited accuracy. The best cutoff for Liver/Spleen HU was 0.84, which yielded an accuracy of 82.5%, precision of 0.784, recall of 0.707, and F1-score of 0.744.

We also evaluated performance across the broader steatosis spectrum. In detecting any hepatic steatosis (score  $\geq 1$ ), Liver/Spleen HU achieved an AUC of 0.739 (**Supplementary Figure 2A**). For severe steatosis (score  $\geq 3$ ), the AUC was 0.763 (**Supplementary Figure 2B**). In both scenarios, Liver/Spleen HU performed comparably or better than CAP, PDFF, and BMI.



## Prediction of Fibrosis Severity

Advanced fibrosis was defined as stage  $\geq 3$  on histology. Traditional fibrosis indices such as LSM (AUC = 0.874) and FIB-4 (0.743) maintained high accuracy. We also evaluated a composite metric, the adjusted visceral fat index ( $VFI - 0.44 \times VFV$ ), which demonstrated an AUC of 0.715 (**Figure 3C**), suggesting that fat distribution may reflect fibrotic progression. The best cutoff was  $-48.15$ , yielding an accuracy of 67.7%, precision of 0.410, recall of 0.732, and an F1-score of 0.526. Additionally, adjusted VFI was tested for its ability to detect significant fibrosis (stage  $\geq 2$ ), yielding an AUC of 0.672 (**Supplementary Figure 2C**). While performance was modest compared to LSM (0.847) and FIB-4 (0.718), adjusted VFI remained independently informative, reinforcing its potential for fibrosis risk stratification.

## Prognostic Value for Liver-Related Events

We assessed the prognostic value of DeepCatch-derived metrics in predicting LREs, defined as a composite of ascites, variceal bleeding, hepatic encephalopathy, hepatorenal syndrome, or liver transplantation. Kaplan–Meier analysis revealed significant LRE-free survival differences stratified by body composition metrics (**Figure 4**). Higher skeletal muscle area was associated with reduced LRE risk, highlighting the protective role of muscle preservation. Similarly, higher skeletal muscle attenuation, indicative of better muscle quality, was also linked to improved outcomes. Conversely, lower adjusted VFI was associated with reduced LRE risk, underscoring the detrimental impact of excessive visceral fat. These results support the relevance of CT-based body composition profiling for long-term risk prediction in MASLD.

Both skeletal muscle area and attenuation were significantly associated with lower LRE risk in crude Cox regression models. The hazard ratio for skeletal muscle area was 0.24 (95% CI: 0.09–0.65,  $p = 0.0046$ ), and for skeletal muscle attenuation, it was 0.37 (95% CI: 0.15–0.88,  $p = 0.0247$ ), reinforcing their protective roles in clinical outcomes, as shown in **Supplementary Table 1**.

## Discussion

In this study, we evaluated the utility of CT-based body composition metrics derived from the DeepCatch software in characterizing the spectrum of MASLD—from steatosis to fibrosis—and in predicting long-term liver-related events. By automatically extracting adipose tissue, skeletal muscle, and organ-specific parameters from routine CT images, DeepCatch-derived metrics were shown to be valuable noninvasive biomarkers across multiple diagnostic and prognostic endpoints, including disease classification, steatosis severity, fibrosis staging, and liver-related event-free survival.

MASLD presents ongoing diagnostic and risk stratification challenges in clinical practice, particularly when distinguishing progressive forms such as MASH or identifying patients at risk for fibrosis-related complications. While transient elastography and MRI-based techniques such as CAP and PDFF are increasingly used, their limited accessibility and higher cost reduce their applicability in routine care. Moreover, traditional indices like BMI and FIB-4 may underperform in patients with altered fat distribution or sarcopenia. Our findings suggest that DeepCatch-derived metrics—particularly visceral fat area, liver-to-spleen attenuation ratio, skeletal muscle area, and the adjusted visceral fat index—may offer meaningful, scalable alternatives for MASLD phenotyping.

Among the endpoints assessed, DeepCatch metrics demonstrated the strongest diagnostic performance for steatosis severity. Liver-to-spleen HU achieved the highest AUC (0.815) for detecting moderate-to-severe steatosis, surpassing commonly used tools such as CAP, PDFF, and BMI. In contrast, while adjusted visceral fat index showed promise in fibrosis staging (AUC = 0.715), its performance was more modest than for steatosis. This discrepancy may be partly attributed to the inverse-U-shaped distribution of fat-based features across the MASLD spectrum. In cirrhosis, hepatic steatosis often regresses due to hepatocyte loss and fibrotic

remodeling, which can obscure the signal captured by fat metrics and reduce predictive accuracy in advanced fibrosis, in contrast to fibrosis-specific markers such as LSM.

The prognostic analysis reinforced the relevance of body composition phenotypes in long-term outcomes. Higher skeletal muscle area and attenuation—reflecting preserved muscle mass and quality—were associated with lower risk of liver-related events. Similarly, lower adjusted visceral fat index values were also protective, underscoring the importance of maintaining muscle integrity and minimizing visceral adiposity as prognostic factors in MASLD.

Several limitations should be noted. The retrospective single-center design may limit the generalizability of the findings, and biopsy, while used as the diagnostic gold standard, is subject to inherent sampling variability. Additionally, our analysis was based on baseline imaging alone; the role of longitudinal changes in body composition over time warrants further study. External validation in prospective multicenter cohorts will also be necessary to confirm the clinical utility of DeepCatch metrics.

In conclusion, CT-derived body composition metrics obtained via DeepCatch offer robust, noninvasive tools for the diagnosis and monitoring of MASLD. While particularly strong in steatosis assessment, fat-based metrics showed more modest performance in fibrosis prediction, likely reflecting biological shifts in advanced disease. Nevertheless, their demonstrated prognostic value for liver-related events highlights their potential for integration into risk stratification models, advancing personalized management strategies in hepatology.

## References

1. Younossi, Z.M., M. Kalligeros, and L. Henry, *Epidemiology of metabolic dysfunction-associated steatotic liver disease*. Clinical and Molecular Hepatology, 2025. **31**(Suppl): p. S32-S50.
2. Abdelhameed, F., et al., *Non-invasive Scores and Serum Biomarkers for Fatty Liver in the Era of Metabolic Dysfunction-associated Steatotic Liver Disease (MASLD): A Comprehensive Review From NAFLD to MAFLD and MASLD*. Current Obesity Reports, 2024. **13**(3): p. 510-531.
3. Chowdhury, A.B. and K.J. Mehta, *Liver biopsy for assessment of chronic liver diseases: a synopsis*. Clinical and Experimental Medicine, 2023. **23**(2): p. 273-285.
4. Ballestri, S., et al., *Diagnostic accuracy of ultrasonography for the detection of hepatic steatosis: an updated meta-analysis of observational studies*. Metabolism and Target Organ Damage, 2021. **1**(1): p. N/A-N/A.
5. Zoncapè, M., A. Liguori, and E.A. Tsochatzis, *Non-invasive testing and risk-stratification in patients with MASLD*. European Journal of Internal Medicine, 2024. **122**: p. 11-19.

**Figure 1.** Study Cohort Flowchart

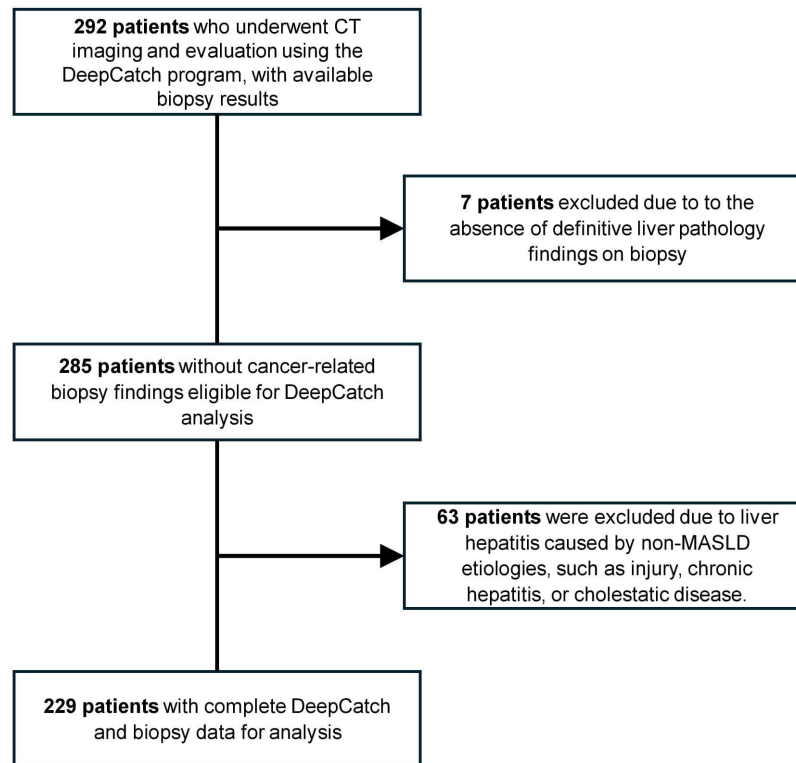


**Figure 2.** Boxplot Analysis of Traditional Metrics and Deepcatch-Derived Metrics Across MASLD Subtypes

(A) Liver Stiffness Measurement (LSM)

(B) Fibrosis-4 Index (FIB-4)

(C) Body Mass Index (BMI)

(D) Controlled Attenuation Parameter (CAP)

(E) Visceral Fat Area

(F) Liver/Spleen HU

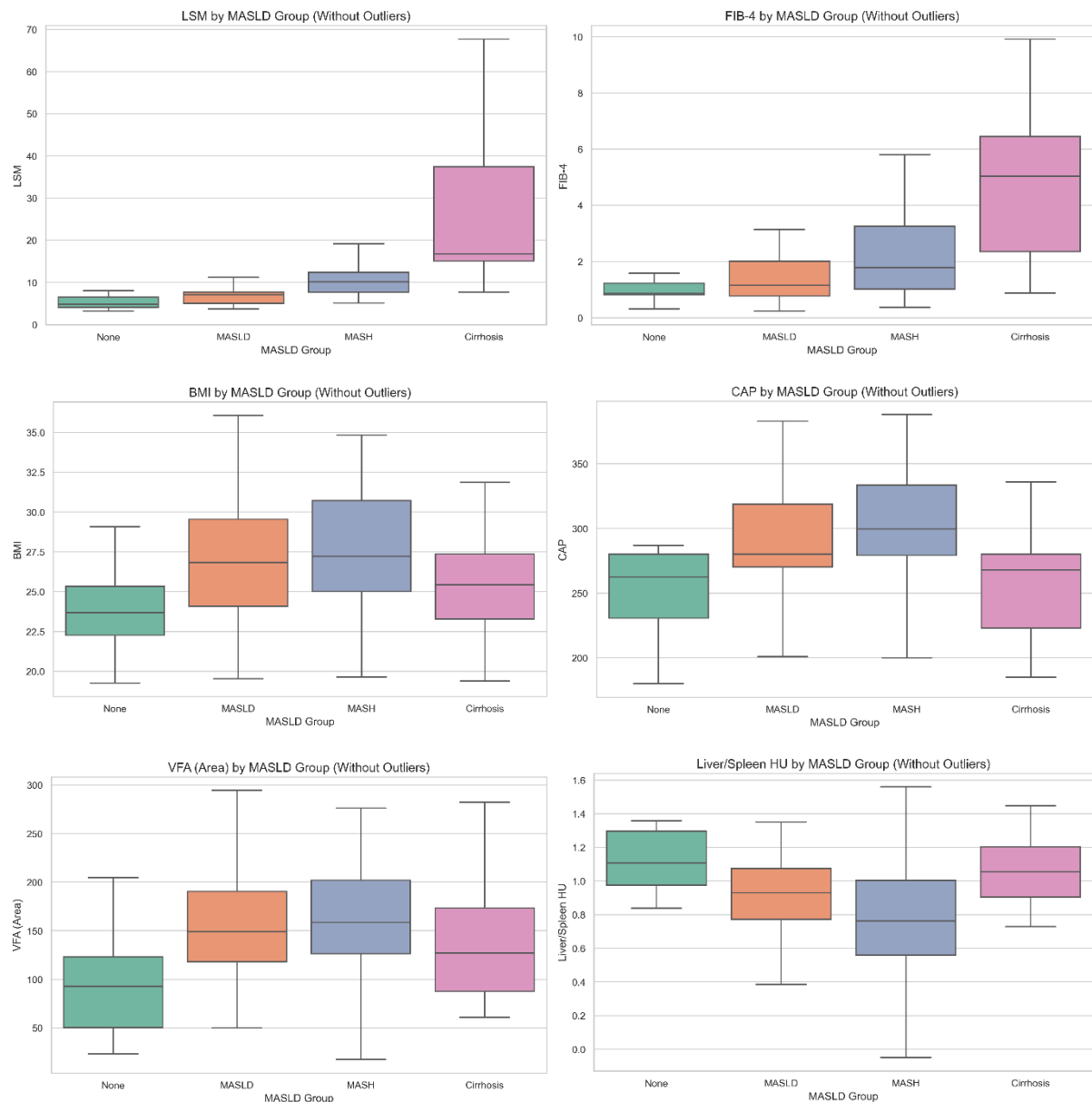
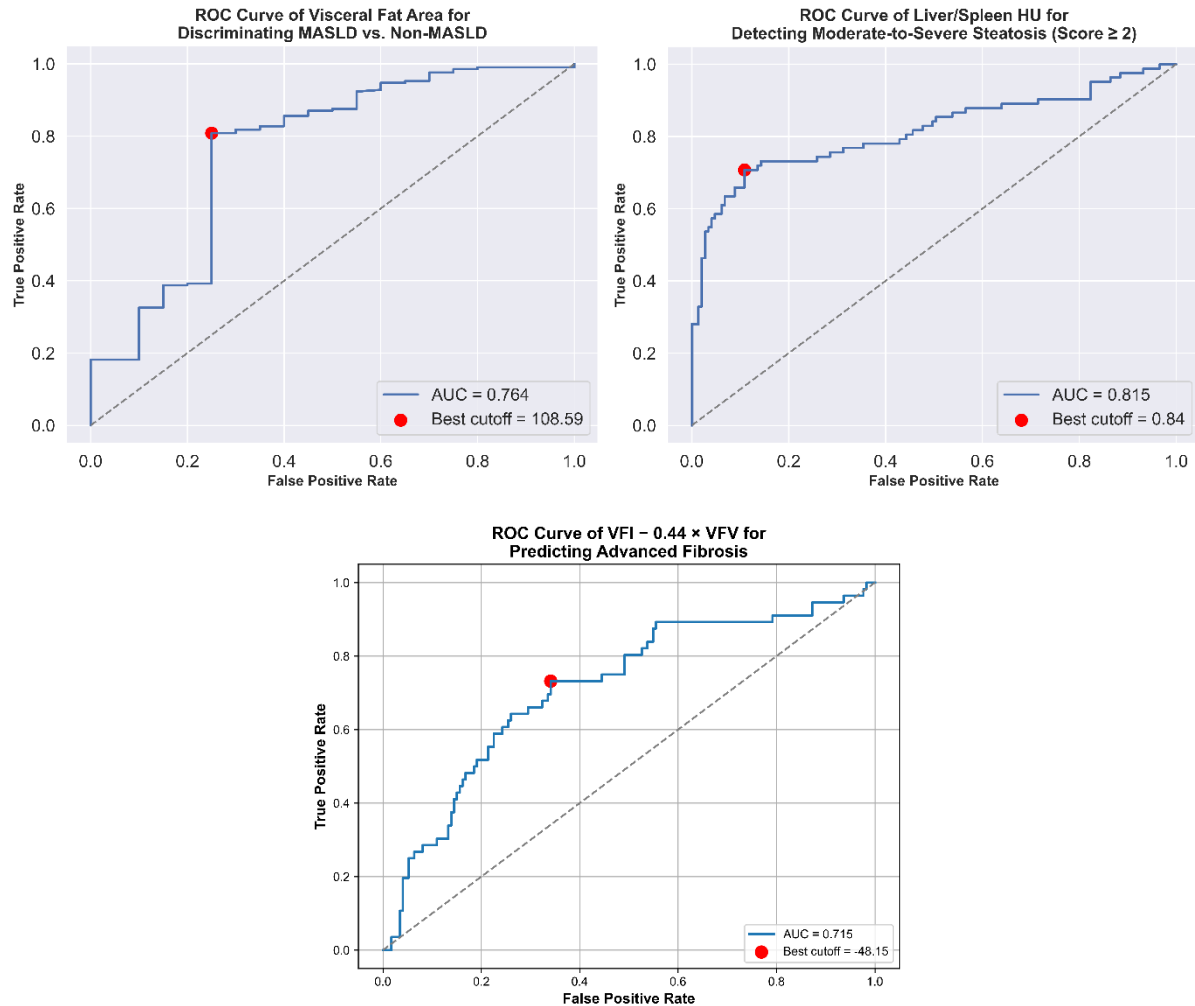


**Figure 3.** ROC Curves of DeepCatch-Derived Metrics for Assessing MASLD Type, Steatosis Severity, and Advanced Fibrosis

(A) Visceral Fat Area for Identifying MASLD

(B) Liver/Spleen HU for Discriminating Moderate-to-Severe Steatosis (Score  $\geq 2$ )

(C) Adjusted Visceral Fat Index ( $VFI = 0.44 \times VFV$ ) for Advanced **Fibrosis Prediction**



**For Identifying MASLD:** BMI (0.744), BMI (Categorical) (0.733), Liver/Spleen HU (0.739), Visceral Fat Index (0.730), Visceral Fat Volume (0.728), Total Fat Index (0.724), Subcutaneous Fat Area (0.723), CAP (0.720)

**For Discriminating Moderate-to-Severe Steatosis:** Liver (HU) (0.771), Liver (PDFF) (0.769), CAP (0.714), BMI (0.599), BMI (Categorical) (0.581)

**For Predicting Advanced Fibrosis:** LSM (0.874), LSM (Categorical) (0.864), FIB-4 (0.743), FIB-4 (Categorical) (0.733), PLT (0.727)

**Figure 4.** DeepCatch-Derived Metrics for Predicting Liver-Related Event-Free Survival

(A) Kaplan–Meier Curve Stratified by Skeletal Muscle Area

(B) Kaplan–Meier Curve Stratified by Skeletal Muscle Attenuation

(C) Kaplan–Meier Curve Stratified by Adjusted Visceral Fat Index ( $VFI - 0.44 \times VFV$ )

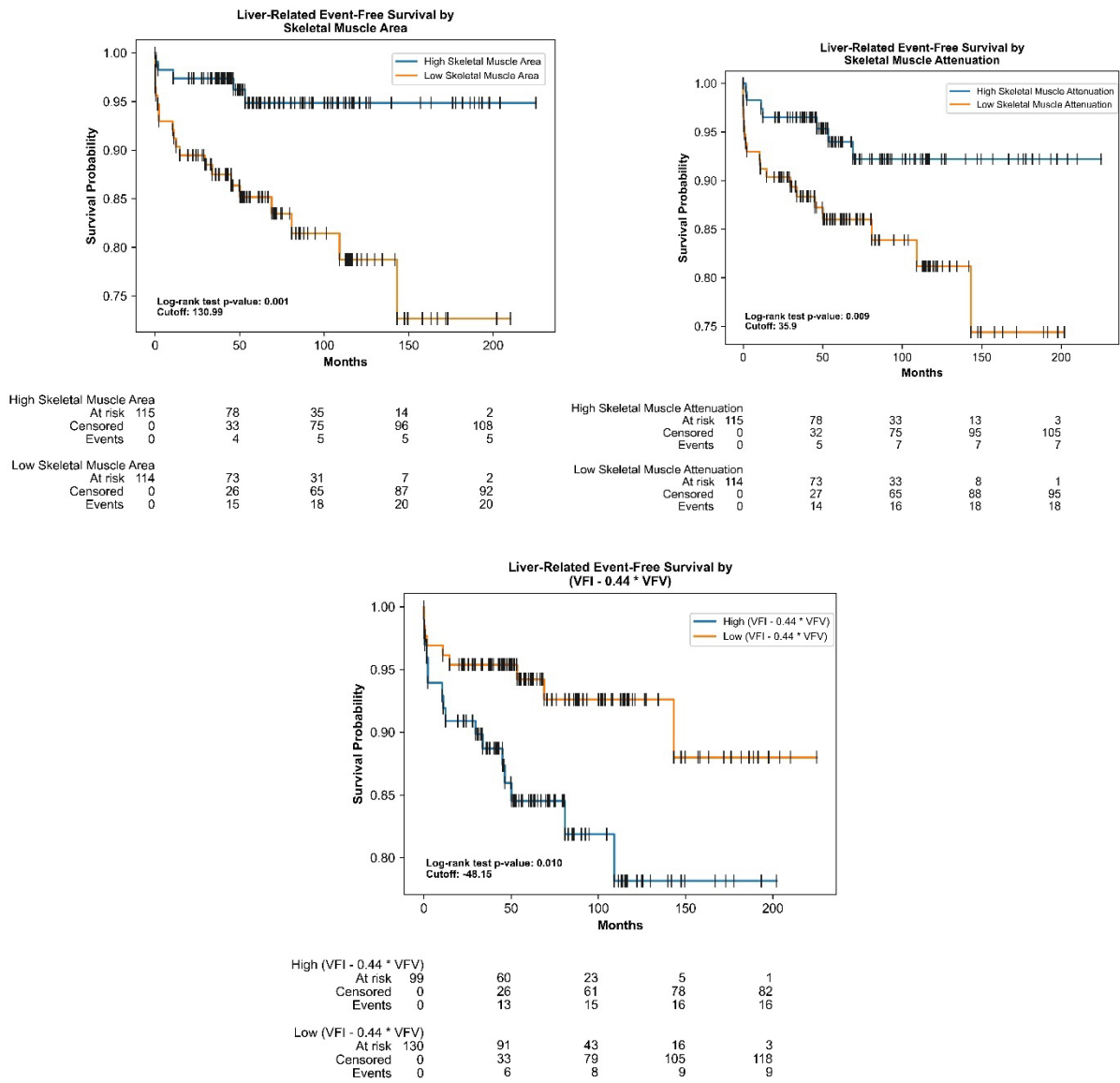




**Table 1.** Baseline Characteristics of Patients by Fibrosis Stage

	<b>Total Patients (n=229)</b>	<b>Advanced Fibrosis Patients <sup>a</sup> (n=56)</b>	<b>Non-Advanced Fibrosis Patients <sup>b</sup> (n=173)</b>	<b><i>P</i></b>
<b>Age, yrs</b>	56.0 (45.0-67.0)	64.0 (48.8-70.2)	54.0 (44.0-65.0)	0.002
<b>Weight, kg</b>	72.0 (63.2-81.7)	67.2 (59.5-75.3)	73.8 (64.3-82.4)	0.004
<b>Height, cm</b>	165.0 (158.0-173.0)	160.0 (153.7-167.2)	167.0 (160.0-174.0)	0.000
<b>Waist to Height Ratio</b>	5.5 (5.1-6.0)	5.6 (5.3-6.0)	5.4 (5.1-6.0)	0.189
<b>BMI, kg/m<sup>2</sup></b>	910.2 (841.9-973.4)	910.8 (838.1-963.4)	910.2 (844.9-983.8)	0.630
<b>VFI, cm<sup>3</sup>/m<sup>2</sup></b>	26.4 (24.0-29.5)	26.3 (23.8-29.0)	26.4 (24.0-29.5)	0.589
<b>SFI, cm<sup>3</sup>/m<sup>2</sup></b>	375.6 (261.2-535.8)	354.6 (188.8-545.6)	381.2 (264.7-530.7)	0.193
<b>TFI, cm<sup>3</sup>/m<sup>2</sup></b>	515.1 (371.5-753.1)	500.3 (306.7-720.5)	517.3 (384.9-754.0)	0.390
<b>SMI, cm<sup>3</sup>/m<sup>2</sup></b>	890.1 (687.7-1302.8)	901.3 (622.4-1267.1)	890.1 (703.1-1306.1)	0.173
<b>VFV, cm<sup>3</sup></b>	48.0 (42.7-56.0)	45.7 (41.0-51.3)	48.8 (43.0-56.8)	0.049
<b>SFV, cm<sup>3</sup></b>	1032.2 (683.4-1425.2)	894.2 (502.0-1292.5)	1064.1 (759.6-1474.6)	0.029
<b>Spleen Volume, cm<sup>3</sup></b>	1382.3 (1014.8-1922.2)	1246.6 (828.6-1795.6)	1448.7 (1056.7-1951.4)	0.082
<b>VFA (Area), cm<sup>2</sup></b>	199.3 (142.5-291.5)	223.6 (142.0-318.9)	194.4 (143.8-277.9)	0.343
<b>SFA (Area), cm<sup>2</sup></b>	149.4 (111.7-189.5)	142.7 (106.3-175.2)	151.5 (111.7-193.2)	0.209
<b>SMA (Area), cm<sup>2</sup></b>	179.9 (139.9-254.9)	180.7 (139.5-259.8)	177.2 (140.1-252.4)	0.899
<b>VFA (Attenuation), HU</b>	131.0 (107.1-158.7)	115.0 (101.5-133.0)	139.5 (111.5-160.0)	0.002
<b>SFA (Attenuation), HU</b>	-96.8 (-103.6--90.2)	-93.9 (-102.8--84.9)	-97.7 (-103.7--92.1)	0.022
<b>SMA (Attenuation), HU</b>	-101.8 (-109.0--95.2)	-101.3 (-108.4--94.6)	-101.9 (-109.1--95.9)	0.274
<b>Liver/Spleen Volume</b>	35.9 (29.1-42.4)	34.2 (25.4-39.4)	36.2 (30.4-43.4)	0.020
<b>Spleen Volume, cm<sup>3</sup></b>	7.7 (5.7-10.0)	7.0 (4.1-9.2)	7.8 (6.0-10.5)	0.084
<b>Liver/Spleen HU</b>	0.9 (0.7-1.1)	1.0 (0.8-1.1)	0.9 (0.7-1.1)	0.038
<b>Liver HU, HU</b>	46.5 (36.7-56.3)	46.9 (41.5-55.2)	45.1 (36.4-56.3)	0.481
<b>Spleen HU, HU</b>	46.5 (42.7-52.2)	44.9 (39.7-50.7)	47.1 (43.1-52.5)	0.083
<b>Liver (PDFF), %</b>	11.1 (5.8-16.7)	10.1 (5.7-14.5)	11.4 (6.2-16.9)	0.460
<b>LSM, kPa</b>	7.7 (6.1-11.4)	14.0 (9.9-17.1)	7.5 (5.1-7.8)	0.000
<b>CAP, dB/m</b>	280.0 (265.0-319.0)	280.0 (236.8-298.5)	280.0 (268.0-320.0)	0.021
<b>AST, IU/L</b>	43.0 (27.0-77.0)	54.5 (37.5-68.0)	39.0 (26.0-79.0)	0.066
<b>ALT, IU/L</b>	55.0 (28.0-95.0)	45.0 (18.0-76.8)	61.0 (32.0-101.0)	0.034
<b>T.bil, mg/dL</b>	0.7 (0.5-1.1)	0.8 (0.6-1.4)	0.7 (0.5-1.1)	0.009
<b>PLT, x 10<sup>3</sup>/mm<sup>3</sup></b>	227.0 (179.0-283.0)	163.0 (115.0-241.2)	238.0 (199.0-292.0)	0.000
<b>PT INR</b>	1.0 (0.9-1.1)	1.0 (1.0-1.1)	1.0 (0.9-1.0)	0.000

<b>Albumin, g/dL</b>	4.4 (3.8-4.7)	4.2 (3.3-4.7)	4.4 (3.9-4.7)	0.042
<b>Glucose, mg/dL</b>	108.0 (95.0-138.0)	113.0 (97.0-140.0)	106.0 (95.0-136.0)	0.405
<b>HbA1c, %</b>	6.4 (6.3-6.6)	6.4 (6.0-6.9)	6.4 (6.3-6.5)	0.670
<b>eGFR, mL/min</b>	96.7 (84.4-118.7)	95.7 (84.3-116.4)	96.9 (85.0-118.7)	0.716
<b>T.chol, mg/dL</b>	168.0 (136.0-202.0)	156.5 (120.0-191.2)	170.0 (142.0-202.0)	0.018
<b>HDL, mg/dL</b>	44.0 (39.0-48.0)	44.0 (34.5-47.2)	44.0 (40.0-48.0)	0.080
<b>LDL, mg/dL</b>	106.5 (106.5-106.5)	106.5 (104.1-106.5)	106.5 (106.5-113.0)	0.002
<b>TG, mg/dL</b>	137.0 (112.0-181.0)	132.0 (102.8-169.0)	137.0 (121.0-183.0)	0.044
<b>SBP, mmHg</b>	125.0 (116.0-134.0)	127.0 (113.0-134.0)	125.0 (116.0-134.0)	0.908
<b>DBP, mmHg</b>	79.0 (70.0-87.0)	77.5 (70.0-86.2)	79.0 (70.0-87.0)	0.600
<b>FIB-4</b>	1.4 (0.9-3.0)	2.9 (1.5-5.4)	1.2 (0.8-2.1)	0.000
<b>Sex</b>				0.040
Male	107 (46.7)	19 (33.9)	88 (50.9)	
Female	122 (53.3)	37 (66.1)	85 (49.1)	
<b>MASLD Type <sup>c</sup></b>				0.000
None	20 (8.7)	0 (0.0)	20 (11.6)	
MASLD	114 (49.8)	0 (0.0)	114 (65.9)	
MASH	70 (30.6)	31 (44.6)	39 (22.5)	
Cirrhosis	25 (10.9)	25 (55.4)	0 (0.0)	
<b>Steatosis Score <sup>d</sup></b>				0.044
0	20 (8.7)	0 (0.0)	20 (11.6)	
1	127 (55.5)	37 (66.1)	90 (52.0)	
2	66 (28.8)	15 (26.8)	51 (29.5)	
3	16 (7.0)	4 (7.1)	12 (6.9)	
<b>Smoking</b>				0.743
Yes	38 (16.6)	8 (14.3)	30 (17.3)	
No	191 (83.4)	48 (85.7)	143 (82.7)	
<b>Liver-Related Event <sup>e</sup></b>				0.000
Yes	25 (11.0)	12 (21.4)	13 (7.5)	
No	204 (89.1)	44 (78.6)	160 (92.5)	
<b>Diabetes/Prediabetes Status</b>				
Diabetes	56 (24.5)	19 (33.9)	37 (21.4)	
Prediabetes	11 (4.8)	4 (7.1)	7 (4.0)	
No	162 (70.7)	33 (58.9)	129 (74.6)	

<b>Hypertension Status</b>				0.042
Yes	60 (26.2)	21 (37.5)	39 (22.5)	
No	169 (73.8)	35 (62.5)	134 (77.5)	
<b>Dyslipidemia Status</b>				0.007
Yes	57 (24.9)	22 (39.3)	35 (20.2)	
No	172 (75.1)	34 (60.7)	138 (79.8)	
<b>Ischemic Heart Disease Status</b>				0.048
Yes	14 (6.1)	7 (12.5)	7 (4.0)	
No	215 (93.9)	49 (87.5)	166 (96.0)	
<b>Cerebrovascular Disease Status</b>				0.428
Yes	10 (4.4)	4 (7.1)	6 (3.5)	
No	219 (95.6)	52 (92.9)	167 (96.5)	
<b>Nephropathy Status</b>				0.183
Yes	10 (4.4)	5 (8.9)	5 (2.9)	
No	219 (95.6)	51 (91.1)	168 (97.1)	

---

<sup>a</sup> Advanced fibrosis was defined as a histologic fibrosis stage of 3 or 4

<sup>b</sup> Non-advanced fibrosis was defined as a histologic fibrosis stage of 0 to 2

<sup>c</sup> MASLD includes both MASLD and probable MASH, while MASH refers to definitive steatohepatitis

<sup>d</sup> Steatosis Score was graded from 0 to 3 based on liver biopsy: 0: < 5% steatosis, 1: 5 – 33% (mild), 2: 34 – 66% (moderate), 3: > 66% (severe)

<sup>e</sup> Liver-Related Event was defined as the first occurrence of any of the following: ascites, variceal bleeding, hepatic encephalopathy, hepatorenal syndrome (HRS), or liver transplantation (LT), confirmed via clinical documentation or imaging.